J. Fluid Mech. (1985), *vol.* 151, *pp.* 443–455
Printed in Great Britain

Relaxation effects observed for turbulent flow over a wavy surface

By JONATHAN ABRAMS AND THOMAS J. HANRATTY
University of Illinois, Urbana, Illinois 61801

(Received 8 March 1984 and in revised form 7 September 1984)

Measurements are presented for different flow rates of the time-averaged wall shear stress and of the root-mean-square value of the turbulent fluctuations along a small-amplitude sinusoidally shaped solid surface. The stresses are found to have a variation along the wave surface which is also sinusoidal. The influence of flow rate and of wavelength on the amplitude and phase angle can be correlated by using a wave-number α^+ made dimensionless with wall parameters.

It is found that for $\alpha^+ > 10^{-2}$ a frozen-turbulence assumption can be made whereby the influence of the wave-induced variation of the mixing length can be ignored. For $\alpha^+ < 10^{-4}$ the flow can be described by assuming the Reynolds stresses are given by an equilibrium assumption. The relaxation from this equilibrium condition is characterized by a sharp change in the phase angle for $6 \times 10^{-4} < \alpha^+ < 10^{-3}$.

This relaxation is associated with physical processes in the viscous wall region which are not yet understood. It is argued that these are principally related to the wave-induced variation of the pressure gradient.

The wave-induced variation of the turbulent fluctuations in the wall shear stress also indicate a relaxation in that the maximum turbulence intensity is located in a region of favourable pressure gradient.

1. Introduction

When a turbulent fluid flows over a sinusoidal solid wave a spatial variation of the pressure and the shear stress will occur at the surface. If the wave is of small enough amplitude a linear response can be expected in that all hydrodynamic variables are described by a single harmonic whose amplitude varies linearly with the wave amplitude.

The critical problem in describing the wave-induced flow is the prediction of the effect of the waves on the turbulence. Two principal differences from flow over a flat surface are that the waves induce large sinusoidal variations in the pressure gradient and in the streamline curvature close to the surface. At present no completely satisfactory methods are available to deal with these effects.

In previous work from this laboratory (Thorsness, Morrisroe & Hanratty 1978; Zilker, Cook & Hanratty 1977) it was shown that measurements of the shear-stress variation along a solid wavy surface provide a particularly sensitive test of turbulence models for the viscous wall region. Results obtained by Thorsness *et al.* (1978) could be described by the modified van Driest model used by Loyd, Moffat & Kays (1970). The most interesting aspect of this model is that it predicts a relaxation whereby the turbulence processes in the viscous wall layer change from a frozen to an equilibrium condition over a small range of dimensionless wavenumbers $\alpha^+ = 2\pi\nu/\lambda v^*$, where v^* is a friction velocity defined using the wavelength-averaged wall shear stress $\langle \bar{\tau}_w \rangle$.

Experimental results were, however, at values of α^+ that are too large to verify this prediction of a sharp relaxation.

This paper presents new measurements of the shear-stress variation along a small-amplitude wavy surface, which cover a wide enough range of α^+ to examine this relaxation effect. They were obtained in a rectangular channel, 5.08 cm high and 61 cm wide, far enough downstream that the flow was fully developed. The bottom wall contained a train of solid waves with the same dimensions used by Thorsness *et al.* The wavelength was 5.08 cm and the amplitude a, equal to half the peak-to-crest distance, was 0.0356 cm. The range of α^+ was extended by studying a wider range of liquid flow rates.

Measurements were made of the variation along the wave surface of the time-averaged velocity gradient and of the root mean square of the turbulent fluctuations in the velocity gradient. This was done by using an electrochemical technique developed in this laboratory by Reiss & Hanratty (1962, 1963) and by Mitchell & Hanratty (1966).

2. Interpretation

The profile of the wave surface that was studied can be represented in Cartesian coordinates as

$$Y_s = a\cos(\alpha X). \tag{1}$$

The presence of such a boundary causes a periodic variation of the time-averaged velocity field, and of the pressure $\bar{p}_w$ and shear stress $\bar{\tau}_w$ at the wall. For a linear response,

$$\bar{\tau}_w = \langle\bar{\tau}_w\rangle + a|\hat{\tau}_w|\cos(\alpha X+\theta_\tau), \tag{2}$$

$$\bar{p}_w = \langle\bar{p}_w\rangle + a|\hat{p}_w|\cos(\alpha X+\theta_p). \tag{3}$$

Here $a|\hat{\tau}_w|$, $a|\hat{p}_w|$ are the amplitudes of the wave-induced stress variations at the wall and θ_τ, θ_p are the number of degrees by which the maxima precede the wave crest.

The variation of $\bar{\tau}_w$ along the wave surface is calculated by solving the linear momentum equations. For this purpose, a boundary-layer coordinate system is used in which the x-coordinate is parallel to the wave surface and the y-coordinate is perpendicular to it. The wave profile is represented as

$$Y_s = a\,e^{i\alpha x}, \tag{4}$$

and a stream function

$$\psi = \int_0^y \langle\bar{U}(y)\rangle\,dy + aF(y)\,e^{i\alpha x}, \tag{5}$$

with $\langle\bar{U}(y)\rangle$ being the velocity profile measured for a flat surface, is defined so that the time-average velocities in the x- and y-directions are given by

$$\bar{U} = h_y^{-1}\frac{\partial\psi}{\partial y}, \quad \bar{V} = -h_x^{-1}\frac{\partial\psi}{\partial x}, \tag{6}$$

where h_x and h_y are the linearized metric functions for the boundary-layer coordinate system:

$$h_x = 1 + a\alpha^2 y\,e^{i\alpha x}, \quad h_y = 1. \tag{7}$$

From the x and y momentum balances the following equation is obtained for F:

$$\mathrm{i}\alpha\left[\langle\bar{U}\rangle\left(\frac{\mathrm{d}^2F}{\mathrm{d}y^2}-\alpha^2F\right)-\frac{\mathrm{d}^2\langle\bar{U}\rangle}{\mathrm{d}y^2}F+\alpha^2\langle U\rangle^2\right]$$
$$=\nu\left[\frac{\mathrm{d}^4F}{\mathrm{d}y^4}-2\alpha^2\frac{\mathrm{d}^2F}{\mathrm{d}y^2}+\alpha^4F+2\alpha^2\frac{\mathrm{d}^2\langle\bar{U}\rangle}{\mathrm{d}y^2}-\alpha^4\langle\bar{U}\rangle\right]+\mathscr{R}. \quad (8)$$

The terms on the left-hand side are the inertia terms associated with the wave-induced flow, with $\alpha^2\langle\bar{U}\rangle^2$ representing a centripetal acceleration associated with the use of a curvilinear coordinate system. The terms in the brackets on the right-hand side arise because of viscous stresses. The term $\mathscr{R}$ contains the wave-induced variation of the Reynolds stresses r_{xx}, r_{xy} and r_{yy}:

$$\mathscr{R}=\mathrm{i}\alpha^3\langle r_{xx}\rangle-\mathrm{i}\alpha^3\langle r_{yy}\rangle+3\alpha^2\frac{\mathrm{d}\langle r_{xy}\rangle}{\mathrm{d}y}+\mathrm{i}\alpha\left(\frac{\mathrm{d}\hat{r}_{xx}}{\mathrm{d}y}-\frac{\mathrm{d}\hat{r}_{yy}}{\mathrm{d}y}\right)+\alpha^2\hat{r}_{xy}+\frac{\mathrm{d}^2\hat{r}_{xy}}{\mathrm{d}y^2}, \quad (9)$$

with
$$r_{ij}=a\hat{r}_{ij}\,\mathrm{e}^{\mathrm{i}\alpha x}+\langle\bar{r}_{ij}\rangle. \quad (10)$$

Equation (8) is solved subject to the boundary condition of zero velocity at the wave surface,

$$F=\frac{\mathrm{d}F}{\mathrm{d}y}=0 \quad \text{at } y=0, \quad (11)$$

and the condition of parallel flow far from the surface,

$$F=\langle\bar{U}\rangle, \quad \frac{\mathrm{d}F}{\mathrm{d}y}=\frac{\mathrm{d}\langle\bar{U}\rangle}{\mathrm{d}y} \quad \text{at large } y. \quad (12)$$

From the solutions of (8), the wall shear stress and pressure can be calculated since, at $y=0$:

$$\frac{\bar{p}_{\mathrm{w}}}{\rho}=-\frac{a\mathrm{i}\nu}{\alpha}\left[\frac{\mathrm{d}^3F(0)}{\mathrm{d}y^3}+\alpha^2\frac{\mathrm{d}^2\langle\bar{U}(0)\rangle}{\mathrm{d}y^2}\right]\mathrm{e}^{\mathrm{i}\alpha x}, \quad (13)$$

$$\frac{\bar{\tau}_{\mathrm{w}}}{\rho}=\frac{\langle\bar{\tau}_{\mathrm{w}}\rangle}{\rho}+a\nu\frac{\mathrm{d}^2F(0)}{\mathrm{d}y^2}\mathrm{e}^{\mathrm{i}\alpha x}. \quad (14)$$

The principal problem in solving (8) is the specification of $\mathscr{R}$. We have used a mixing-length model to describe the turbulent stresses:

$$r_{ij}=-\tfrac{1}{3}q^2\delta_{ij}+\nu_{\mathrm{T}}2\bar{S}_{ij}, \quad (15)$$

$$\nu_{\mathrm{T}}=l^2|2\bar{S}_{ij}|, \quad (16)$$

$$l=l_0=\kappa y[1-\exp(-D_{\mathrm{M}})], \quad (17)$$

$$D_{\mathrm{M}}=y\bar{\tau}^{\frac{1}{2}}\rho^{\frac{1}{2}}/\mu A, \quad (18)$$

with $\bar{S}_{ij}$ being the rate-of-strain tensor. The effect of streamline curvature can be taken into account by modifying the mixing-length in a manner suggested by Bradshaw (1973):

$$l=l_0(1-\beta_{\mathrm{c}}Ri_{\mathrm{c}}). \quad (19)$$

Here β_{c} is an empirical constant and Ri_{c} is the curvature Richardson number defined as

$$Ri_{\mathrm{c}}=\frac{2\bar{U}}{R_{\mathrm{c}}\dfrac{\partial\bar{U}}{\partial y}}, \quad (20)$$

with $1/R_{\mathrm{c}}$ being the curvature of the streamlines.

The term κ is the von Kármán constant and the argument of the exponential term in (17) is a damping factor which allows for a rapid decrease of the mixing length in the viscous wall region. For equilibrium boundary layers Loyd *et al.* (1970) suggest the following functional dependence of A on pressure gradient:

$$A = 25\left[1 + k_1\left(\frac{\mu}{\rho^{\frac{1}{2}}\tau_w^{\frac{3}{2}}}\frac{\mathrm{d}\bar{P}_w}{\mathrm{d}x}\right) + \ldots\right], \tag{21}$$

with $k_1 = -30$. Equation (21) makes use of the concept that turbulence in the viscous wall region is enhanced in unfavourable pressure gradients and decreased in favourable pressure gradients.

For small-amplitude waves with negligible effects of curvature an equilibrium assumption can be made for very small α:

$$\hat{\tau}_{ij} = 2\langle\nu_T\rangle\hat{s}_{ij} + 2\hat{\nu}_T\langle\bar{S}_{ij}\rangle, \tag{22}$$

$$\hat{\nu}_t = \langle\bar{\nu}_t\rangle\left[\frac{\hat{s}_{ij}}{\langle\bar{S}_{ij}\rangle} + \frac{2\hat{l}_0}{\langle\bar{l}_0\rangle}\right], \tag{23}$$

$$\hat{l}_0 = \kappa y \exp\left(\frac{-y\rho^{\frac{1}{2}}\langle\bar{\tau}\rangle^{\frac{1}{2}}}{25\mu}\right)\hat{d}_M, \tag{24}$$

$$\hat{d}_M = \frac{y\rho^{\frac{1}{2}}\langle\bar{\tau}\rangle^{\frac{1}{2}}}{25\mu}\left[\frac{\hat{\tau}}{2\langle\bar{\tau}\rangle} - \frac{\mathrm{i}\alpha^+ k_1\hat{p}_w}{\langle\bar{\tau}\rangle}\right]. \tag{25}$$

It is noted from (24) that wave-induced variations of the mixing length $\hat{l}_0$ are only important in the viscous wall region. Within the framework of the van Driest equation these effects are interpreted as a thickening or thinning of the viscous wall region caused by wave-induced variations of the shear stress and of the pressure gradient.

For very large α^+ the wave-induced variations of the flow are confined to a region close to the wave surface. If α^+ is large enough this region is so thin that viscous stresses dominate over turbulent stresses and a quasi-laminar assumption can be made, $\langle\hat{\tau}_{ij}\rangle = 0$. However, a less restrictive assumption can be made if it is assumed that certain aspects of the turbulence are frozen. In particular, this concept is applied only to the viscous wall region by assuming at large α^+ that

$$\hat{l}_0 = 0, \tag{26}$$

$$\hat{\tau}_{ij} = 4\langle\nu_t\rangle\hat{s}_{ij}. \tag{27}$$

It is assumed that the relaxation from an equilibrium to a frozen condition is described by a single rate constant. At intermediate α it is argued that an effective wave-induced damping function, $\hat{d}_{Meff}$ rather than $\hat{d}_M$, should be used in the momentum equations. This is represented by a simple first-order rate equation

$$\frac{\mathrm{d}}{\mathrm{d}x}(D_{Meff}) = \frac{D_M - D_{Meff}}{k_D}, \tag{28}$$

where k_D is the relaxation constant. From (28) one obtains

$$\hat{d}_{Meff} = \frac{\hat{d}_M}{1 + \mathrm{i}\alpha^+ k_D^+}. \tag{29}$$

For large values of $\alpha^+ k_D^+$, $\hat{d}_{Meff} = 0$ and (29) represents a frozen turbulence ($\hat{l}_0 = 0$)

model. For $\alpha^+ k_D^+$ very small, $\hat{d}_{Meff} = \hat{d}_M$ and (29) represents an equilibrium situation. In the range of α^+ given by

$$\alpha^+ k_D^+ \approx 1, \tag{30}$$

a change from an equilibrium to a frozen condition is initiated.

Our experiments have involved the measurement of the variation of the time-averaged wall shear stress, $\bar{\tau}_w(x)$, and of the root-mean-square value of the turbulent fluctuations, $\tau'_w(x)$, for different values of the dimensionless wavenumber α^+.

3. Description of the experiments

The flow loop, sketched in figure 1, was originally built by Cook (1970) and later modified. The principal change that had to be made for the experiments described in this paper is the installation of new pumping capacity and of large-diameter piping in order to obtain larger flows, up to 170 l/s. The rectangular flow channel has a cross-section of 5.08×61 cm and a length of 838 cm.

Provision was made to replace a 68.6 cm length of the bottom wall at the downstream end of the channel with a wall containing a train of ten waves. The waves were cut into a rectangular section of Plexiglas using specially designed cutting tools.

The pattern of 0.635 mm holes shown in figure 2 was drilled into the wave section. Platinum electrodes, 0.508 mm in diameter, were epoxyed into these holes. When the epoxy was dry, the portions of the wires protruding from the surface were filed flush with the surface. The surface was then smoothed with progressively finer grades of sandpaper and polishing compounds. On completion of the polishing, the profile of the waves was measured using a dial indicator.

The shear-stress measurements were made over the sixth, eighth and ninth waves. No differences were observed in the measurements obtained from these three waves. Figure 3 shows the measured profile for the ninth wave. The amplitude of each wave was obtained by doing a least-squares fit of a sine wave to the profile. Information on the profiles of the other waves, together with a detailed description of the method of fabrication, is contained in a thesis by one of the authors (Abrams 1984).

The platinum wires flush with the wave surface were cathodes in an electrolysis cell. An electrolyte, 0.0015 M in I_3^- and 0.2 M in KI, was circulated through the system. A potential difference was established between the cathode and the anode and the following reactions occurred:

$$I_3^- + 2e^- \rightarrow 3I^- \qquad \text{(cathode)},$$

$$3I^- \rightarrow I_3^- + 2e^- \qquad \text{(anode)}$$

At a high enough voltage the reaction rate at the cathode was so rapid that the concentration of I_3^- at the cathode surface was zero and the current I flowing through the electrolysis circuit was controlled by the rate of mass transfer of I_3^- to the cathode surface. Under these conditions the time-averaged current $\bar{I}$ was related to the time-averaged wall shear stress by the equation

$$\bar{I} = C\bar{\tau}_w^{\frac{1}{3}}. \tag{31}$$

The fluctuations in the current were related to the fluctuations in the shear stress as follows:

$$\frac{I - \bar{I}}{\bar{I}} = \frac{1}{3}\frac{\tau'_w}{\bar{\tau}_w}. \tag{32}$$

The constant in (31) was calculated from physical properties of the electrolyte and

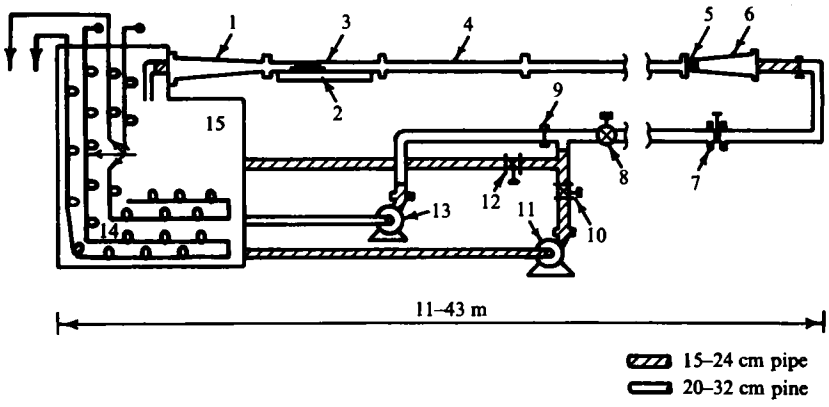

FIGURE 1. Equipment used in the study of flow over solid wavy surfaces. 1, Downstream rectangular to round diffuser; 2, removable wave surface; 3, test section; 4, channel; 5, honeycomb; 6, upstream rectangular to round diffuser, 7, annubar flow meter; 8, butterfly throttling valve; 9, removable blanking plate; 10, diaphragm valve; 11, small pump; 12, by-pass diaphragm valve; 13, large pump; 14, cooling coils; 15, reservoir tank.

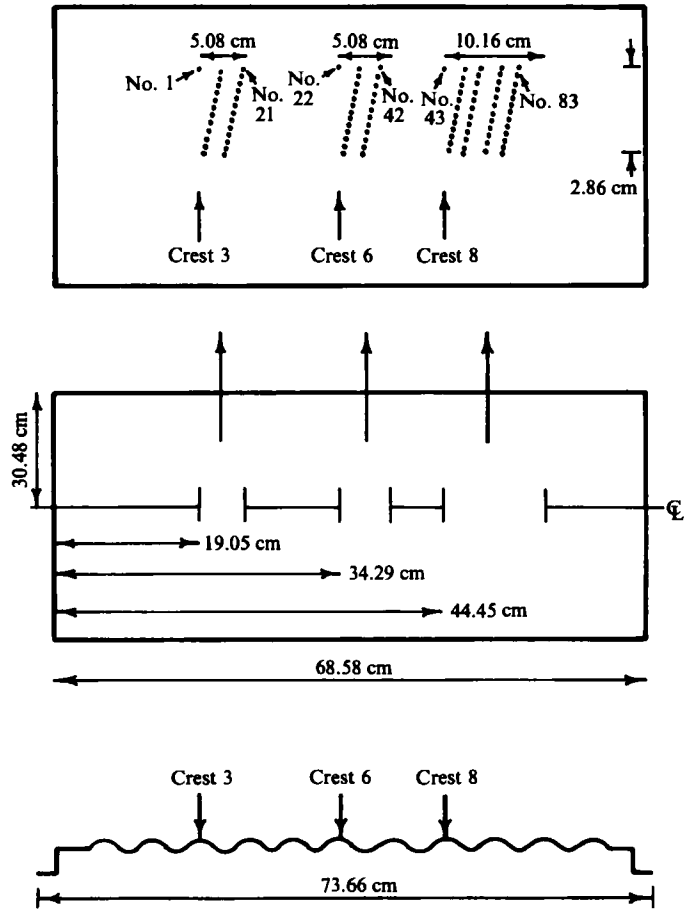

FIGURE 2. Pattern of holes for the electrodes.

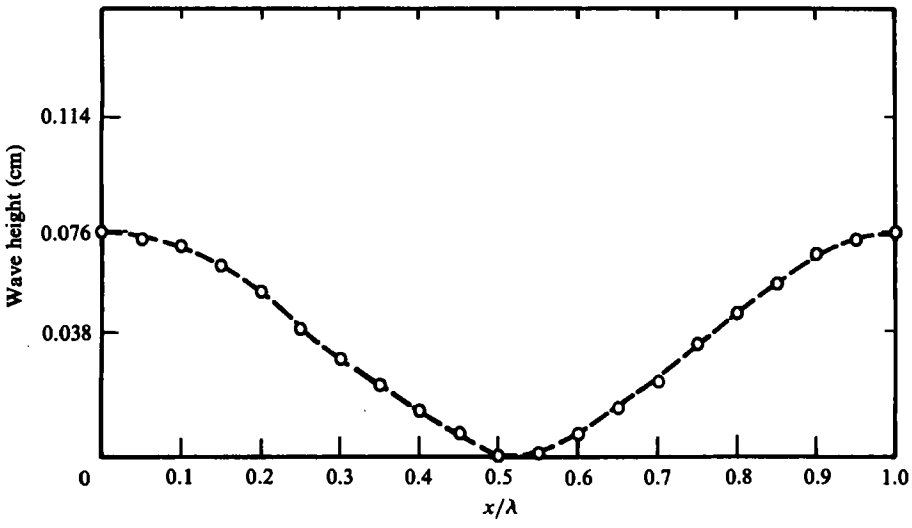

FIGURE 3. Wave profile.

the measured area of the test electrode from the following equation given by Mitchell & Hanratty (1966):

$$C = 0.807 \frac{D n_e F A_e C_B}{L} \left(\frac{L^2}{\mu D}\right)^{\frac{1}{3}}. \tag{33}$$

Here D is the diffusion coefficient, F Faraday's constant, n_e the number of electrons involved, A_e the electrode area, C_B the bulk concentration of the reacting species and L the effective electrode length.

The electronic equipment used to measure the current and other details regarding this technique are given in a review article by Hanratty & Campbell (1983).

Values of the pressure gradient in the channel with a flat wall for the test section, reported by Thorsness *et al.* (1978), are in good agreement with literature values. Velocity measurements made over a flat wall for $y^+ \geqslant 30$ obtained by Zilker (1976) for large flow rates exhibit the logarithmic behaviour

$$\frac{\bar{U}}{v^*} = \frac{1}{0.41} \ln (y^+) + 5.1 \tag{34}$$

suggested by Kline, Morkovin & Cockrell (1969).

The meter used to measure flow rates was calibrated by integrating these measured velocity profiles. A bulk velocity is defined as if the velocity profile at the centre of the channel existed over the whole cross-section:

$$U_b = \frac{1}{h} \int_0^h \bar{U} \, dy, \tag{35}$$

where h is the half-width of the channel and $\bar{U}$ is the average velocity at a distance y from the surface. The Reynolds number used to characterize the flow is then

$$Re = \frac{h U_B}{\nu}. \tag{36}$$

Typical measured profiles of $\bar{\tau}_w/\langle \bar{\tau}_w \rangle$ and of $(\tau_w'^2)^{\frac{1}{2}}/\langle \bar{\tau}_w \rangle$ are shown in figure 4. The solid lines represent a least-square fit of a sinusoidal curve to the data. It is to be

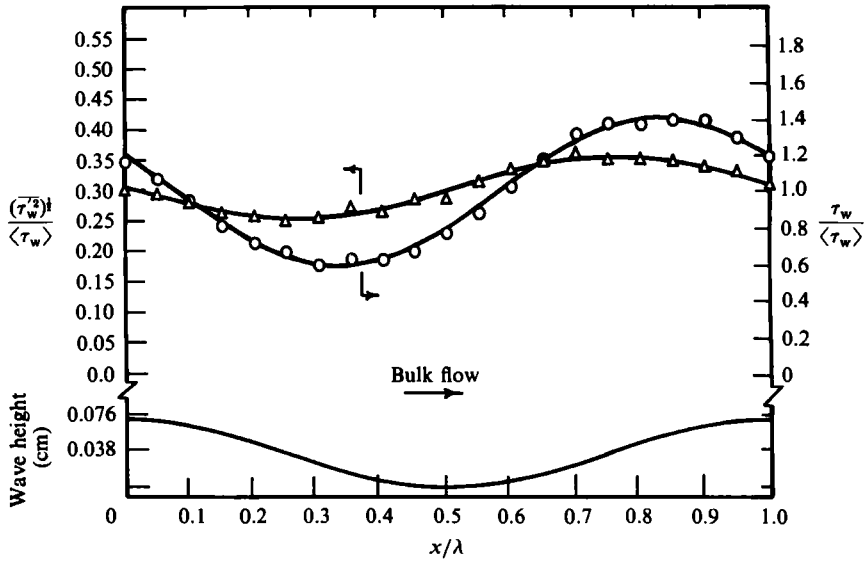

FIGURE 4. Typical measurements of the mean wall shear stress $\bar{\tau}_w/\langle\bar{\tau}_w\rangle$ and the root mean square of the fluctuations in the wall shear stress $\overline{(\tau_w'^2)}^{\frac{1}{2}}/\langle\bar{\tau}_w\rangle$, for $\alpha^+ = \alpha\nu/v^* = 0.00566$.

noted that the maximum in both cases is upstream of the wave crest. From this least-squares fit, the amplitudes and the phase angles characterizing the spatial variation of the wall shear stress and the fluctuations in the wall shear stress are calculated.

4. Results

4.1. *Measurements of* $\bar{\tau}_x(x)$

The phase angles θ_τ and the amplitudes $|\hat{\tau}_w|$, made dimensionless using $\langle\bar{\tau}_w\rangle$ and the friction length ν/v^*, are plotted against the dimensionless wavenumber α^+ in figures 5 and 6. The results on θ_τ fall into a range of α^+ where neither the frozen turbulence nor the equilibrium model predict the phase angle. For $\alpha^+ > 0.003$ the amplitude agrees with predictions using a frozen-turbulence assumption, but the values of α^+ covered in the experiments were too large to observe equilibrium behaviour.

The most striking result is the sharp decrease in the phase angle Θ_τ in the range of $\alpha^+ = 6\times10^{-4}$–$10^{-3}$. Previous experiments from this laboratory (Thorsness *et al.* 1978) covered the range $\alpha^+ = 0.002$–0.01 and therefore did not indicate this relaxation phenomenon. Our most recent experiments covered the range $\alpha^+ = 6\times10^{-4}$–$10^{-2}$. In the region of overlap with previous work excellent agreement is noted. Also there is reasonably good agreement with results obtained by Kendall (1970), Hsu & Kennedy (1971) and Sigal (1970).

The relaxation theory with $k_D^+ = 1650$ and $k_1 = -33$ describes the measured phase angle and amplitude of the wall shear-stress variation quite well. It is noted that in the range $0.000\,15 < \alpha^+ < 0.002$ the theory not only predicts the observed sharp change in Θ_τ but also the observed low values of $|\hat{\tau}_w|$, compared to the equilibrium model or the frozen-turbulence model. This fit of the relaxation model enables us to extrapolate our measurements. From this extrapolation we find that the equilibrium

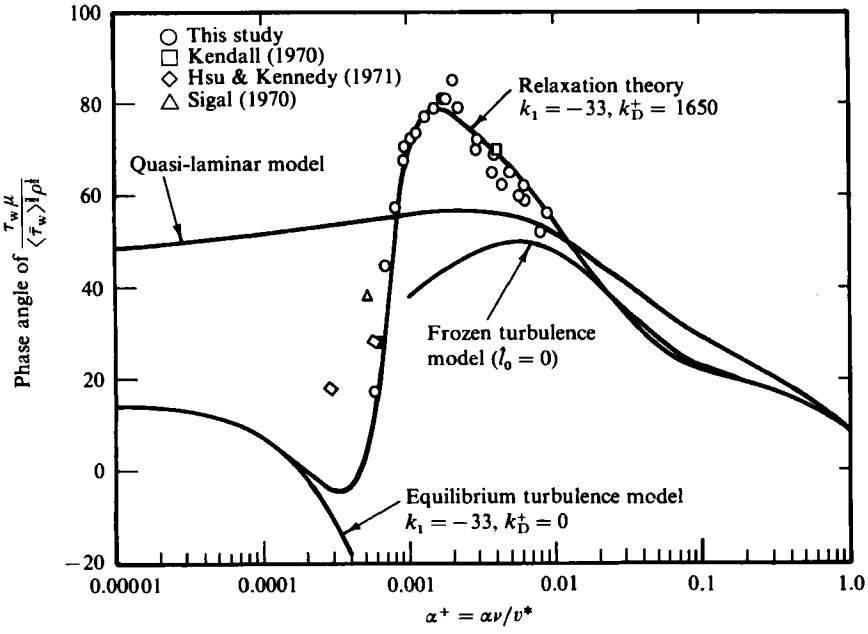

FIGURE 5. The phase angle characterizing the variation of the wall shear stress as a function of the dimensionless wavenumber.

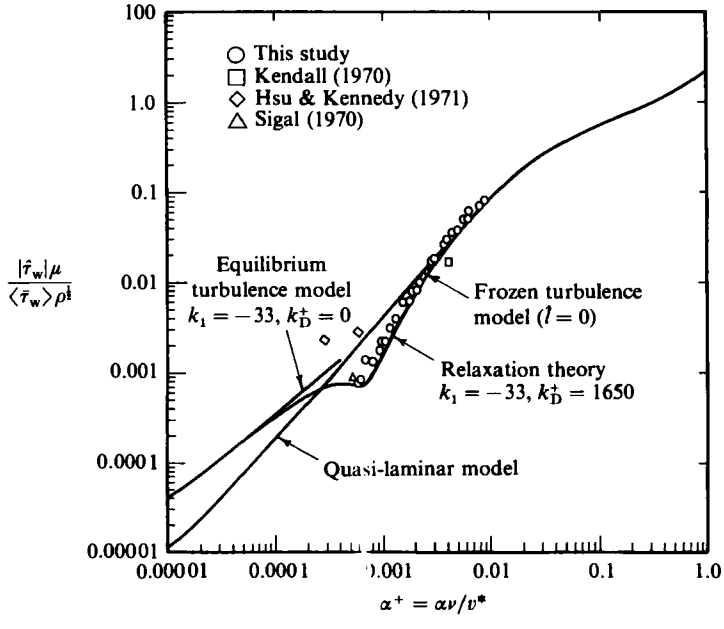

FIGURE 6. The amplitude characterizing the variation of the wall shear stress as a function of the dimensionless wavenumber.

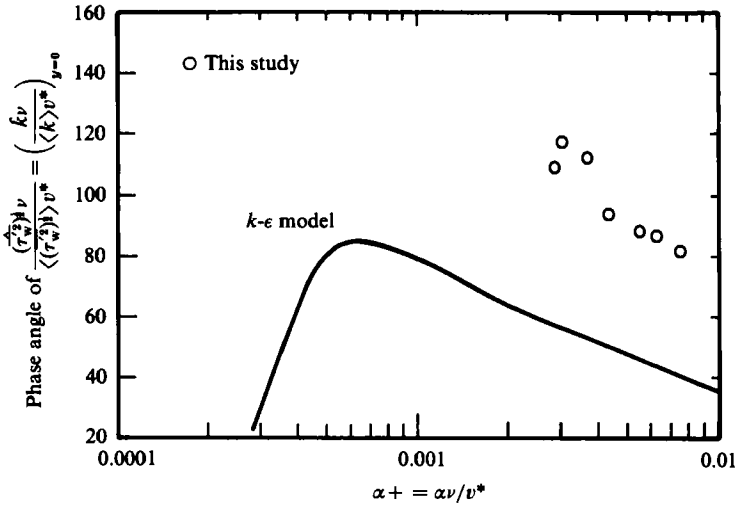

FIGURE 7. Measured phase angles characterizing the variation of the root mean square of the fluctuations in the wall shear stress.

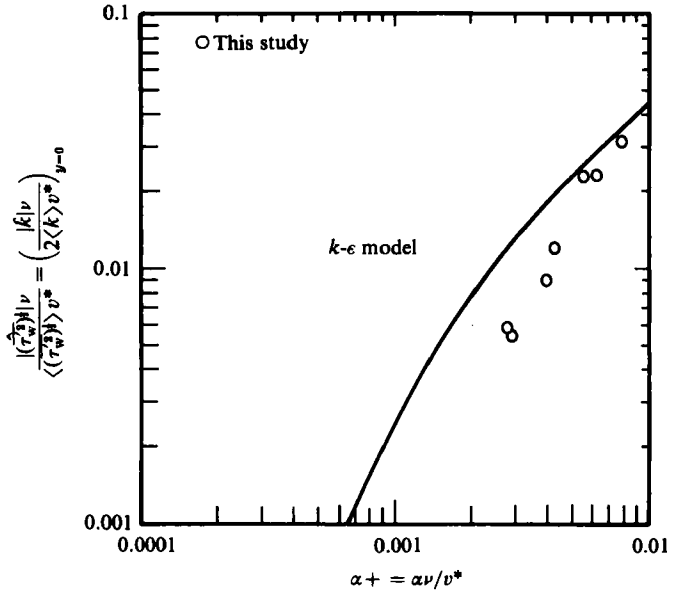

FIGURE 8. Measured amplitudes characterizing the variation of the root mean square of the fluctuations in the wall shear stress.

model will be valid for $\alpha^+ < 10^{-4}$ and that the frozen-turbulence model is valid for $\alpha^+ > 2 \times 10^{-2}$. It is also to be noted from figure 5 that the quasi-laminar assumption describes the phase angles only for $\alpha^+ > 0.6$.

4.2. *Measurements of* $\overline{(\tau_w'^2)^{\frac{1}{2}}}$

The phase angles and amplitudes characterizing the measured variation of $\overline{(\tau_w'^2)^{\frac{1}{2}}}$ with x are shown in figures 7 and 8. It is noted that the amplitude decreases strongly with decreasing α^+. In fact it became so small that measurements could not be made for $\alpha^+ < 0.0025$.

The most noteworthy aspect of these results is that the maximum in the wave-induced variation occurs in a region of favourable pressure gradient. This is the opposite of what would be expected for an equilibrium situation and, consequently, is another manifestation of the relaxation of the turbulence observed for $\alpha^+ > 0.00015$.

Also of interest are the large values of the wave-induced variation of turbulent shear-stress fluctuations at $\alpha^+ \approx 0.01$, where a quasi-laminar model appears to give good agreement between predicted and measured values of $|\hat{\tau}_w|$ (see figure 6). This would suggest that, if a completely frozen turbulence assumption is strictly applicable, much larger values of α^+ than 0.01 would be required. This is one of the reasons why we chose to describe our measurements by relaxing only the wave-induced variation $\hat{l}_0$ in the mixing length. However it is likely, as pointed out by Thorsness *et al.* (1978), that there is a large range of α^+ for which $\hat{\tau}_{ij} \neq 0$ but for which inertia effects and viscous stresses are much larger than turbulence stresses so that the assumption of $\hat{\tau}_{ij} = 0$ gives good results, even though it is not correct.

More measurements at values of α^+ larger than 0.01 are clearly needed. However, it should be pointed out that the interpretation of the measurements presented in this paper is not affected by relaxing between an equilibrium condition and a quasi-laminar condition (as was done in the thesis by Abrams 1984), instead of between an equilibrium condition and a frozen mixing-length assumption (as is done here).

5. Discussion

The most important contribution of this paper is the demonstration of a relaxation phenomenon which occurs for flow over a wavy surface for $\alpha^+ > 0.00015$. Thorsness *et al.* (1978) have already demonstrated that wave-induced variations in the Reynolds stresses for $y^+ > 40$ have little effect on $\bar{\tau}_w(x)$ for $\alpha^+ > 0.00015$. Consequently it is assumed that this relaxation is a property of physical processes in the viscous wall region.

In figure 9 we compare our measured values of Θ_τ to calculations in which the influence of wave-induced variations of the streamline curvature and the influence of pressure gradient on the van Driest viscous length parameter ($k_1 = 0$, $k_D^+ = 1650$) are neglected. Poor agreement is noted. Abrams (1984) has shown that streamline curvature can have only a small effect on $\bar{\tau}_w(x)$. Consequently, we conclude that the observed relaxation effect is associated with the wave-induced variation of the pressure gradient; i.e. a non-zero value of k_1 is needed.

We recognize that the method used to describe the effect we observed is not satisfactory. This is particularly true with the empirical manner in which relaxation effects are introduced. In this sense a two-equation model, of the k-ϵ type, is more satisfactory. The influence of pressure gradient then comes about because of its influence on the shear-stress variation and, therefore, the turbulence production. Thus relaxation is introduced in a more natural way. However, we have found that presently available formulations of the k-ϵ model do not adequately describe our measurements.

This is shown in figures 9 and 10, where we compare calculations of $\bar{\tau}_w(x)$ using the modification of the Jones & Launder (1973) formulation presented by Chen (1980) to measurements. The dependence of Θ_τ and $|\hat{\tau}_w|$ on α^+ are not properly represented.

No measurements were made of the z-component of the turbulent shear-stress fluctuations at the wavy wall. For turbulent flow over a flat plate the neglect of the z-component of the turbulent velocity fluctuations would introduce only a 10% error

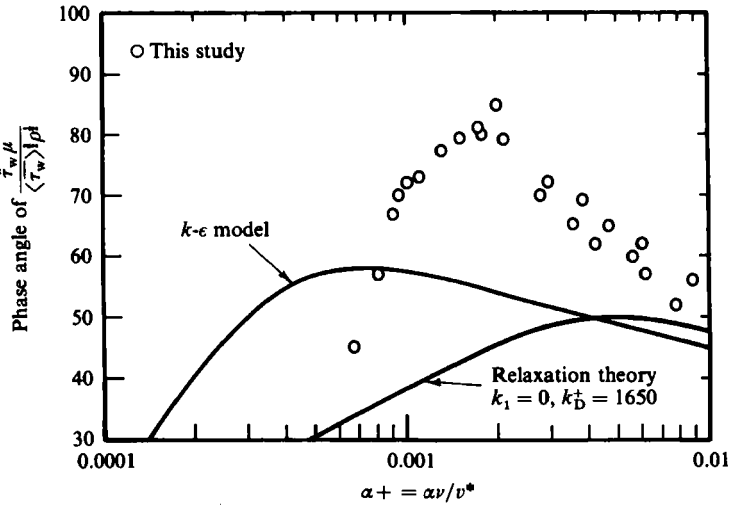

FIGURE 9. Comparison of measurements of the phase angle characterizing the variation of the wall shear stress with various models.

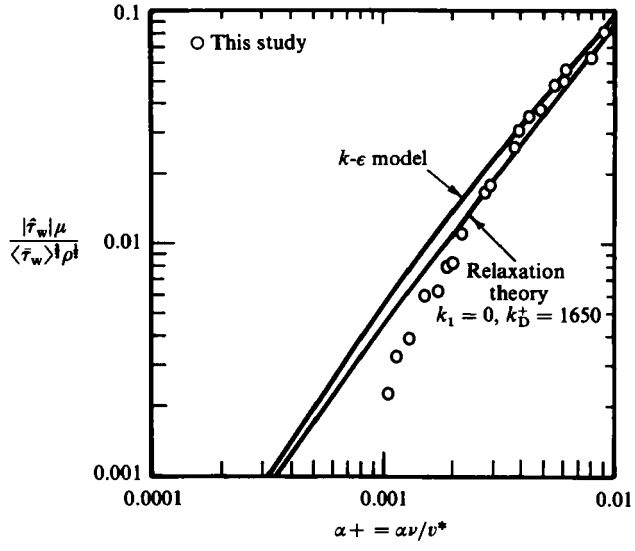

FIGURE 10. Comparison of measurements of the amplitude characterizing the variation of the wall shear stress with various models.

in the calculation of the turbulent kinetic energy k close to the wall. Consequently, measurements of $\overline{(\tau_w'^2(x))^{\frac{1}{2}}}$ are compared to calculations using the k-ϵ model by assuming that in the immediate vicinity of the wall $k \simeq \frac{1}{2}\overline{u'^2}$. The comparison of the calculated amplitude and phase of the wave-induced variation of the turbulent shear-stress fluctuations with measurements, shown in figure 7 and 8, gives some interesting similarities. Large values of the amplitude of turbulent fluctuations are calculated at large α^+ and the calculated phase angles indicate that the maximum energy occurs in a region of favourable pressure gradient.

This work is being supported by the ONR under Grant N00014-88-82-12-0324 by the Shell Companies Foundation.

REFERENCES

ABRAMS, J. 1984 Turbulent flow over small amplitude solid waves. Ph.D. thesis, Department of Chemical Engineering, University of Illinois, Urbana.

BRADSHAW, P. 1973 Effects of streamline curvature and buoyancy in turbulent shear flow. *AGARDograph* No. 169.

CHEN, K. Y. 1980 Prediction of channel and boundary layer flows with a low Reynolds number two-equation model of turbulence. *AIAA* 80-034.

COOK, G. W. 1970 Turbulent flow over solid wavy surfaces. Ph.D. thesis, Department of Chemical Engineering, University of Illinois, Urbana.

HANRATTY, T. J. & CAMPBELL, J. A. 1983 Measurements of wall shear stress. In *Fluid Mechanics Measurements* (ed. R. J. Goldstein), p. 559. Hemisphere.

HSU, S. & KENNEDY, J. F. 1971 *J. Fluid Mech.* **47**, 481.

JONES, W. P. & LAUNDER, B. E. 1973 *Intl J. Heat Mass Transfer* **16**, 1119.

KENDALL, J. M. 1970 *J. Fluid Mech.* **41**, 259.

KLINE, S. J., MORKOVIN, M. V. & COCKRELL, D. J. 1969 *Comp. Turbulent Boundary Layers: 1968 AFOSR-IFP-Stanford Conf. Thermosci. Div., Stanford University.*

LOYD, R. J., MOFFAT, R. J. & KAYS, W. M. 1970 *Thermosci. Div. Stanford Univ. Rep.* HMT-13.

MITCHELL, J. W. & HANRATTY, T. J. 1966 *J. Fluid Mech.* **26**, 199.

REISS, L. P. & HANRATTY, T. J. 1962 *AIChE J.* **8**, 245.

REISS, L. P. & HANRATTY, T. J. 1963 *AIChE J.* **9**, 154.

SIGAL, A. 1970 An experimental investigation of the turbulent boundary layer over a wall. Ph.D. thesis, Department of Aeronautical Engineering, Cal. Inst. Tech.

THORSNESS, C. B., MORRISROE, P. E. & HANRATTY, T. J. 1978 *Chem. Engng Sci.* **33**, 579.

ZILKER, D. P., COOK, G. W. & HANRATTY, T. J. 1977 *J. Fluid Mech.* **82**, 29.